Journal of Vacuum Science & Technology B

Photoluminescence Lifetime of Perovskites on Modified Substrates

Running title: Photoluminescence Lifetime of Perovskites on Modified Substrates

Running Authors: Vorhies, X. et al.

Xavier Vorhies,[1,2] Jessica M. Andriolo,[1,2] Joseph J. Thiebes,[3] Emma K. Orcutt,[3] Erik M. Grumstrup,[3] and Jack L. Skinner[1,2]

1Mechanical Engineering, Montana Technological University, Butte, MT 59701

2Montana Tech Nanotechnology Laboratory, Montana Technological University, Butte, MT 59701

3Chemistry and Biochemistry, Montana State University, Bozeman, MT 59717

a) Electronic mail: xvorhies@mtech.edu

I. ABSTRACT

Lead halide perovskites have gained attention for their potential in optoelectronic applications, including photovoltaics and light-emitting devices, due to their remarkable optical and electronic properties. However, performance of these materials is highly dependent on morphological properties of the underlying substrates. In this study, the effects of substrate modifications on the photoluminescence lifetimes of $CsPbBr_3$ perovskites deposited on TiO_2 substrates that were annealed at various temperatures were investigated.

TiO_2 substrates were characterized using glancing-angle X-ray diffraction and spectroscopic ellipsometry to assess changes in crystallinity and surface roughness. Time-correlated single photon counting spectroscopy was employed to measure the photoluminescent lifetimes of the perovskites. SEM and X-ray diffraction were used to determine morphology and crystallinity.

Results show a clear relationship between substrate annealing temperature and the photoluminescent lifetime of perovskite microcrystals. Substrates annealed at temperatures below 300 °C exhibited increased surface roughness with increased annealing temperature (22.4 Å at room temperature and 48.05 Å at 300 °C) and correspondingly shorter photoluminescent lifetimes (3.5 ns at room temperature and 0.4 ns at 300 °C) suggesting more rapid charge carrier recombination. In contrast, substrates annealed at 350 °C exhibited the longest lifetimes at 4.19 ns indicating a decrease in trap-mediated non-radiative recombination. Substrates annealed at 400 °C showed a further increase in crystallinity but did not extend the lifetime beyond that seen at 350 °C, suggesting an optimal balance between surface roughness and crystallization.

These findings provide insights into the role of morphological substrate modifications in optimizing the optoelectronic properties of perovskite materials.

Journal of Vacuum Science & Technology B

II. INTRODUCTION

Lead halide perovskites have emerged as a transformative class of materials for optoelectronic applications due to their remarkable optical and electronic properties.[1,2] Their unique combination of high light absorption coefficients, long carrier diffusion lengths, and tunable bandgaps has made them a material of choice for the development of next-generation solar cells, light-emitting diodes (LEDs), and photodetectors.[3] Perovskite-based solar cells have demonstrated power conversion efficiencies approaching those of traditional silicon-based cells, positioning perovskites as a promising alternative for next-generation solar energy technologies.[4–6]

Stability and performance of perovskite materials remains highly dependent on their interaction with underlying substrates.[7,8] Morphological properties of substrates, such as surface roughness and crystallinity, can directly impact the optoelectronic behavior of the perovskite layer, influencing charge carrier dynamics and device efficiency.[9] For instance, rough substrates can introduce defect states that act as charge carrier traps, reducing device efficiency.[10,11] Conversely, smooth and crystalline substrates can enhance charge carrier mobility as the density of surface defects decreases, reducing the number of non-radiative recombination centers available at the perovskite-substrate interface.[8,12] In theory, a more ordered substrate will provide a smoother, lower defect surface, allowing for enhanced charge carrier mobility and reduced recombination.[13,14] Understanding how morphological substrate characteristics affect the excited state lifetimes at the perovskite-substrate interface is critical for optimizing their performance in practical applications.[11,15]

In this work, we focus on the excited state lifetimes of $CsPbBr_3$ perovskites deposited on TiO_2 substrates that have been modified by various annealing conditions prior to perovskite deposition. Using time-correlated single photon counting (TCSPC) spectroscopy, we examine the relationship between morphological substrate modifications and the photoluminescence (PL) lifetime of perovskites. Previous studies have explored the influence of substrate properties on perovskite performance, but a gap remains in understanding the specific effects of substrate treatments on excited state dynamics.[13,16,17]

Our research provides new insights into the role of substrate optimization on optoelectronic properties of perovskite materials. Findings presented here serve as a foundation for future work aimed at improving the stability and efficiency of perovskite-based devices.

Journal of Vacuum Science & Technology B

III. EXPERIMENTAL

A. Materials

Lead(II) bromide ($PbBr_2$, 99.999% trace metals basis), cesium bromide (CsBr, 99.999% trace metals basis), acetone (≥99.9% HPLC grade), isopropyl alcohol (≥99.5% ACS reagent grade), and dimethyl sulfoxide (DMSO, ≥99.9% ACS reagent grade) were purchased from Sigma-Aldrich. Indium tin oxide (99.95%) and titanium dioxide (99.99%) targets for sputter deposition were purchased from Angstrom Engineering.

B. Substrate Preparation

1. TiO2 Substrate Deposition

Silicon wafers and glass coverslips were cleaned using semiconductor-grade water followed by rinsing with acetone and isopropyl alcohol. Samples were then dried using dry nitrogen.

Transparent TiO_2 substrates were prepared by sputter deposition technique using an Angstrom Engineering Nexdep PVD platform. Indium tin oxide (ITO) and TiO_2 films were sputter-coated onto silicon wafers and glass coverslips. An argon plasma was used as the operating gas with a throw distance to the substrate of approximately 13 cm. Operating parameters are detailed in Table I. The thicknesses of the deposited films were 100 nm for ITO and 60 nm for TiO_2, as confirmed by profilometry.

Table I: Operating parameters used for sputter deposition of thin film substrates onto silicon wafers and glass coverslips.

Sputter Target	**Target Diameter (in)**	**Operating *Pressure (mTorr)***	***Power Density* (W/in^2)**	**Deposition *Temperature* (°C)**	**Deposition *Rate* (nm/hr)**
ITO	2	3	17.0	21-24	23
TiO_2	2	3	14.3	21-23	149

2. Annealing Treatments

Following deposition at room temperature (25 °C), the as-deposited TiO_2 substrates were subjected to annealing at various temperatures to modify the surface properties. The annealing temperatures ranged from 100 to 400 °C, with a ramp rate of 5 °C/min. Substrates were annealed for 1 hr in air at each temperature to promote recrystallization and modify the surface roughness.

3. Surface Characterization

Surface roughness of the annealed substrates was measured using variable angle spectroscopic ellipsometry (VASE), and glancing-angle X-ray diffraction (GAXRD) was employed to determine the crystallographic properties of the TiO_2 films.

C. Perovskite Synthesis

Journal of Vacuum Science & Technology B

1. Solution Preparation

The perovskite solution was prepared using adapted methods from literature. [18–22] A 0.48 M precursor solution of cesium bromide (CsBr) and lead bromide ($PbBr_2$) was prepared by dissolving equal molar ratios of CsBr and $PbBr_2$ in dimethyl sulfoxide (DMSO). The solution was stirred at 48 °C for 4 hr and then filtered using a 0.22 μm syringe filter to remove any particulate impurities. The filtered solution was stored at room temperature prior to use.

2. Substrate Preparation

Oxygen (O_2) plasma treatment was used prior to the deposition of perovskite material to enhance the wettability of the substrate. The substrate was exposed to O_2 plasma at 50 W for 5 min. Afterwards, the substrate was immediately subject to the microcrystalline perovskite deposition process.

3. Deposition of Perovskite Microcrystals

Perovskite microcrystals were synthesized by drop-casting 50 μL of the $CsPbBr_3$ precursor solution onto the TiO_2-coated substrates. The samples were then annealed at 120 °C for 5 min to promote the formation of microcrystalline perovskite structures and drive off remaining solvent.

D. Characterization Techniques

1. Scanning Electron Microscopy (SEM)

The morphology and composition of the perovskite crystals were characterized using scanning electron microscopy (SEM) with energy-dispersive X-ray spectroscopy (EDS). SEM images provided detailed visualizations of the cuboid $CsPbBr_3$ crystals formed on the surface of the modified substrates, while EDS confirmed the elemental composition.

2. X-ray Diffraction (XRD)

X-ray diffraction (XRD) was conducted on the perovskite-coated substrates to verify the presence of crystalline $CsPbBr_3$. GAXRD was used for both the substrate and the perovskite microcrystals to assess any changes in phase due to substrate annealing or perovskite formation.

3. Time-Correlated Single Photon Counting (TCSPC) Spectroscopy

Photoluminescence lifetimes of the perovskites on differently treated substrates were measured using TCSPC. The home-built TCSPC setup was centered around a Ti:sapphire oscillator (Coherent Chameleon, Santa Clara, CA) operating at an 80 MHz repetition rate, with 85 fs pulse duration and a tunable range of 680 to 1040 nm. For these experiments, the oscillator was fixed at 850 nm, producing an excitation wavelength of 425 nm via second harmonic generation using a frequency doubler (APE GmbH, Berlin, Germany). The repetition rate was reduced to 4 MHz using an electro-optic modulator (Conoptics, Danbury, CT). Data acquisition and analysis were performed with a Picoquant PicoHarp 300 and FluoTime 200 software. A long-pass filter was positioned between the sample and detector to eliminate scattered excitation light. The instrument response function (IRF), determined by scattering the excitation beam from a clean soda-lime glass slide, was approximately 200 ps. The resulting decay traces were fitted to a biexponential model, with the IRF incorporated into the convolution of the fit.

Samples were positioned with the coverslip facing the laser for optical measurements. This orientation was chosen such that optical excitation would occur at the perovskite-substrate interface (Figure 1). The resulting decay curves were fitted using biexponential decay models to quantify the lifetime of charge carriers in the perovskite layer.

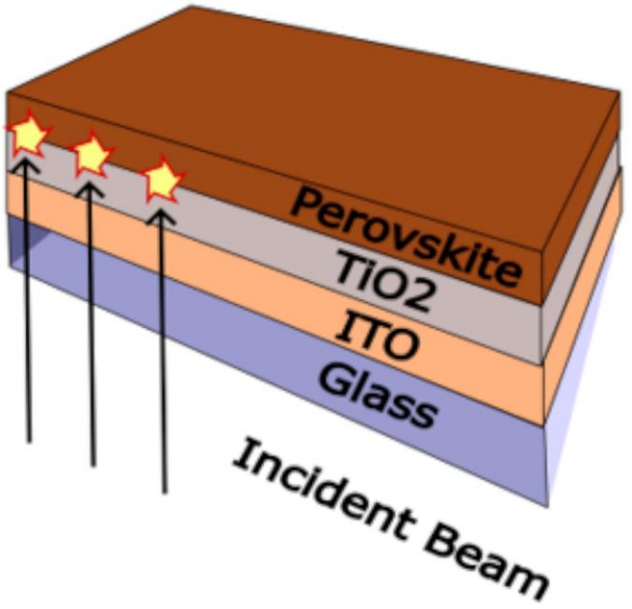

Figure 1: Depiction of sample orientation with respect to incident laser. The depicted orientation was chosen to achieve excitation at perovskite-substrate interface.

4. Profilometry

A Veeco Dektak 3 surface profilometer was utilized to measure the step height and thickness of the deposited ITO and TiO_2 layers on the substrates. The step height was determined by using a scratch-mode test on the surface of the samples, allowing for precise thickness measurement of the deposited films. The thickness of the ITO and TiO_2 layers was measured across multiple points on the substrates to ensure uniformity, with average thicknesses of 100 nm for ITO and 60 nm for TiO_2 confirmed. These measurements were used to verify deposition consistency prior to subsequent processing steps.

5. Atomic Force Microscopy (AFM)

Atomic force microscopy (AFM) was used to obtain topographic visualizations of the TiO_2 layer before the deposition of the perovskite materials. AFM measurements were carried out with a Bruker Dimension Edge in tapping mode using a silicon nitride probe. Scans were performed over a 50 × 50 μm area. These topographic images were used to qualitatively assess changes in surface morphology and uniformity of the substrates following the various annealing treatments.

6. Spectroscopic Ellipsometry

VASE was conducted to obtain precise measurements of the surface roughness of the TiO_2 substrates both before and after the annealing treatments. Measurements were performed using a variable-angle spectroscopic ellipsometer across the wavelength range of 250-1000 nm. The surface roughness of the samples was derived

by using CompleteEASE modeling software. Fitting the ellipsometry data was achieved using two B-Spline layers to represent the TiO_2 on top of an ITO substrate. The best fit model fits a graph to the obtained data, including refractive index of the material, by iterating on various parameters including layer thickness and substrate roughness, as shown in Figure S1 in the supplementary material. Data fitting accurately estimated the thickness of the ITO and TiO_2 layers as previously determined using profilometry. The roughness values were used to evaluate the effect of substrate modification on perovskite growth and charge carrier dynamics.

E. Data Analysis

1. Photoluminescence Decay Fitting

The TCSPC decay curves were analyzed using biexponential fitting to obtain key fitting parameters: fluorescence lifetimes, τ_1 and τ_2, which represent the slow and fast decay components, respectively, and their associated amplitudes A_1 and A_2. The short lifetime arises due to carrier-carrier interactions while the longer lifetime is due to excitonic recombination or trap mediated recombination processes. The results of the biexponential fitting are shown in Table II. The amplitude average lifetimes were calculated using Eq. 1 for each substrate treatment to assess the impact of annealing on the PL lifetime of the perovskite materials. The reported values were compared across various annealing temperatures ranging from room temperature to 400 °C.

Table II: Compiled data from biexponential fitting of TCSPC analysis. Data shows the slow and fast decay components, their reported amplitudes, and the calculated average lifetime. Average lifetime values were determined using Eq.1.

Annealing Temp (°C)	τ_1 (ns)	τ_2 (ns)	Amplitude 1 (A_1)	Amplitude 2 (A_2)	Average Lifetime (ns)
25	7.957	0.729	1961.9	3158.0	**3.50**
100	7.205	0.901	2533.7	2445.3	**3.85**
150	9.658	0.795	1216.1	4228.7	**2.51**
200	3.539	0.173	2765.1	7033.8	**1.11**
250	2.416	0.387	2268.7	5952.5	**1.06**
300	3.456	0.175	1407.8	8288.0	**0.63**
350	8.356	1.419	2092.5	3135.1	**4.19**
400	3.168	0.204	2919.4	6286.0	**1.26**

$$Average\ Lifetime = \frac{\tau_1 A_1 + \tau_2 A_2}{A_1 + A_2} \qquad \text{(Eq. 1)}$$

IV. RESULTS AND DISCUSSION

A. Effect of Substrate Annealing on Surface Properties

GAXRD confirmed that annealing at temperatures below 300 °C did not result in recrystallization of the TiO_2 layer, while substrates annealed at 350 °C and 400 °C exhibited clear recrystallization to the anatase phase (Figure 2). VASE measurements showed that the surface roughness of the TiO_2 films increased with increasing annealing temperature up to 300 °C, but decreased as recrystallization proceeded at higher temperatures where a smoothing effect was more pronounced (Figure 3). This modification of the substrate's morphological properties through annealing influences the optoelectronic behavior of the perovskite-substrate interface.

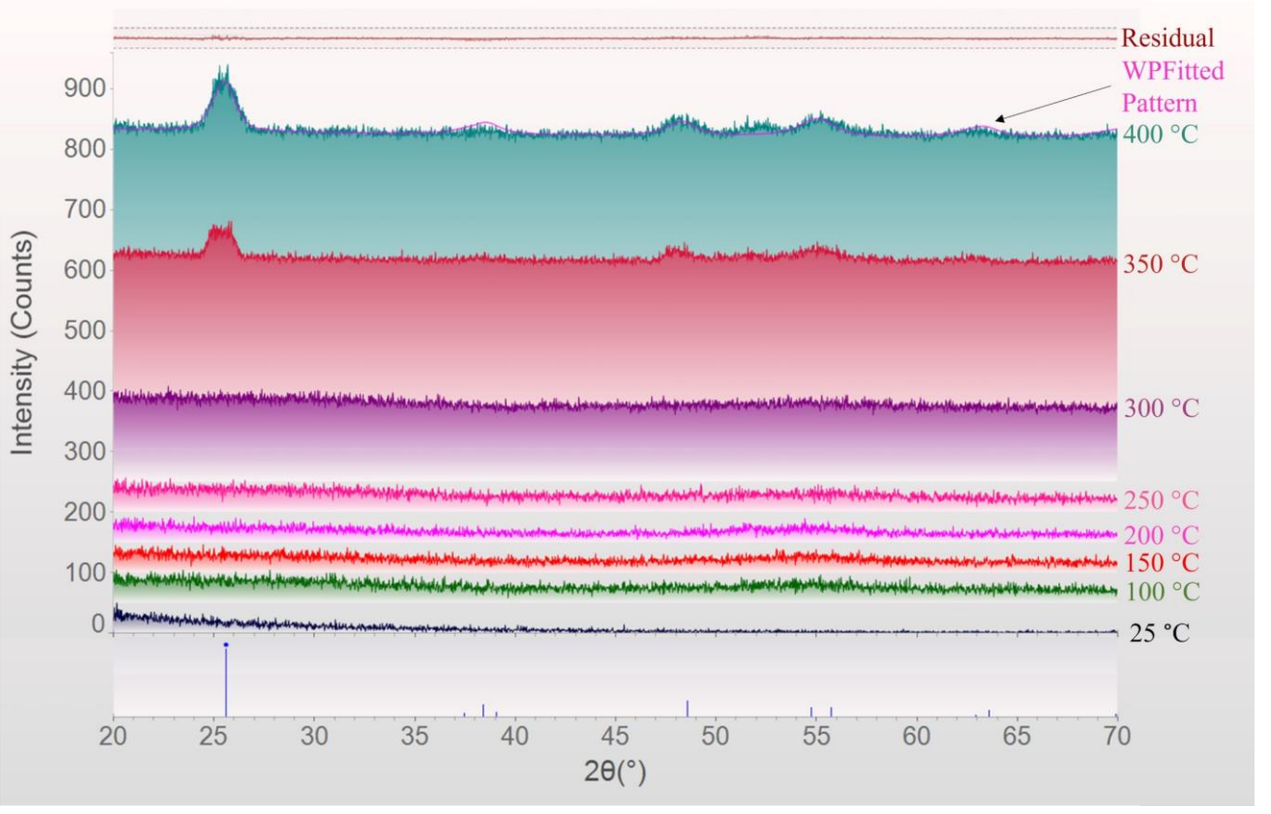

Figure 2: GAXRD analysis of annealed substrates shows recrystallization to the anatase phase at higher temperature treatments (350 – 400 °C). The as-deposited samples were synthesized at room temperature (25 °C). TiO_2 substrate remains amorphous at temperatures 300 °C and below. The X-ray incident angle was fixed at 0.5° for each sample. The Weighted Profile Fitted Pattern (WPFitted Pattern) using the XRD Powder Diffraction File (PDF) 98-000-0081 for TiO2 is shown in pink. The residual error comparing the WPFitted Pattern to the observed pattern for the sample annealed at 400 °C confirms the presence of recrystallized anatase TiO_2.

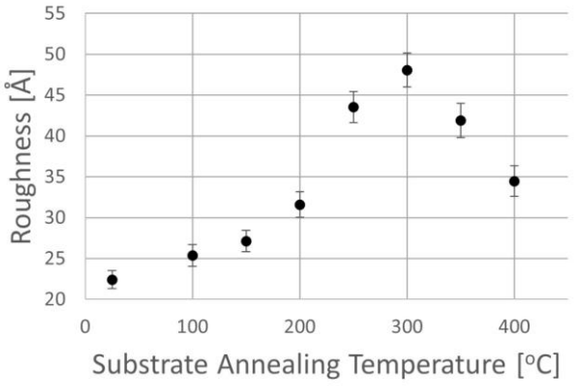

Figure 3: VASE analysis was performed to determine the surface roughness of the substrates due to the various annealing temperatures.

AFM imaging was performed on the TiO_2 coated substrates to assess the topographic uniformity of the samples. As shown in Figure 4, AFM analysis reveals a surface with minimal height variations across the scanned area. This indicates that the sputter deposition of TiO_2 results in a high-quality thin film.

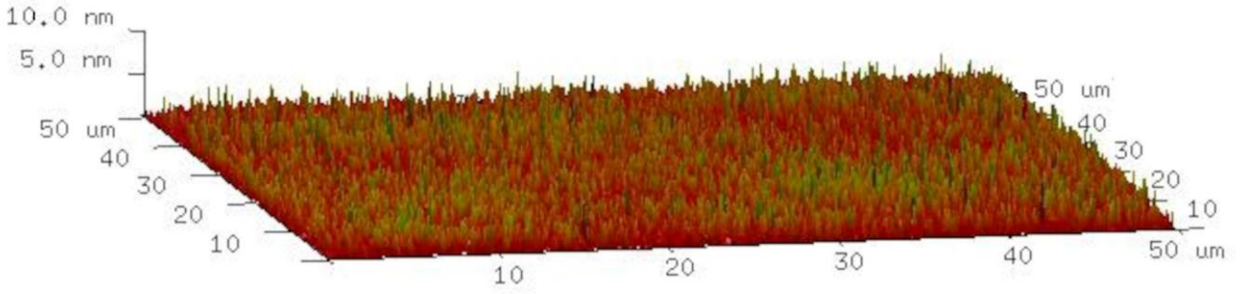

Figure 4: AFM 3D topographic image of the as deposited TiO_2 substrate (25 °C) obtained over a 50 × 50 µm scan area. The data shows smooth surface morphology with minimal height variations across the scanned area. The small variation in height indicates uniformity.

B. Perovskite Morphology and Crystallinity

SEM micrographs revealed that the $CsPbBr_3$ perovskites deposited on TiO_2 substrates formed well-defined cuboid microcrystals (Figure 5). The size of these cuboids ranged from 5 μm to 30 μm in edge length, with heights between 1 μm and 15 μm. EDS confirmed the composition of the crystals as $CsPbBr_3$, consistent with the desired perovskite phase, as shown in Figures S2-3 and Table S1 in the supplementary material. XRD analysis further supported these findings, showing characteristic peaks corresponding to the crystalline $CsPbBr_3$ phase, as shown in Figure S4 in the supplementary material.

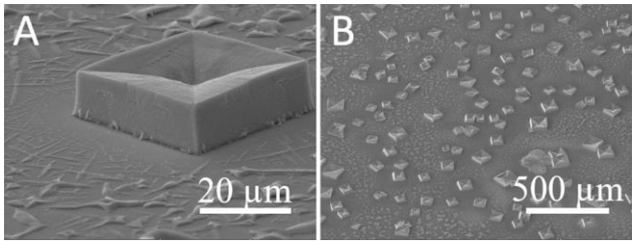

Figure 5: (A)SEM image showing well-formed cuboid structures with visible contact on the substrate. (B) Lower magnification image of the perovskite structure shown in Figure 5A. Further analysis by EDS showed composition indicative of $CsPbBr_3$ perovskites. For each micrograph, the TiO_2 substrate was annealed at 100 °C.

C. Photoluminescence Lifetime of Perovskites on Modified Substrates

TCSPC spectroscopy was employed to study the PL lifetimes of perovskite microcrystals on substrates with varying annealing conditions, as shown in Figures S5-6 in the supplementary material. The biexponential fitting of the TCSPC decay curves yielded two key lifetimes: τ_1, representing slow decay, and τ_2, representing fast decay components, as shown in Figure S7 and Table S2 in the supplementary material. The amplitude average fluorescence lifetime was used to evaluate the overall charge carrier recombination behavior across different substrate treatments.

Data analysis shows that the long lifetime, τ_1, showed greater changes with the annealing treatment of the substrate while the short lifetime, τ_2, showed smaller variations. This result is in agreement with established theory whereby interface engineering has greater influence on the trap-mediated recombination processes.[13,14]

Results indicate that for annealing temperatures ranging from RT to 300 °C, amplitude of average PL lifetime decreases from 3.5 ns at room temperature to 0.63 ns at 300 °C as seen in Figure 6. These results strongly correlate to the increased surface roughness previously reported by VASE. However, at temperatures above 300 °C there is a discontinuity in this behavior due to the recrystallization of the anatase phase at higher temperatures. Perovskites deposited on substrates annealed at 350 °C exhibited the longest amplitude average lifetime of 4.19 ns, indicating that a partially crystalline mixed phase substrate promotes more efficient charge carrier dynamics. Conversely, substrates treated at intermediate temperatures with higher surface roughness and no anatase recrystallization showed shorter lifetimes, indicating faster charge carrier transport into the TiO_2 substrate.

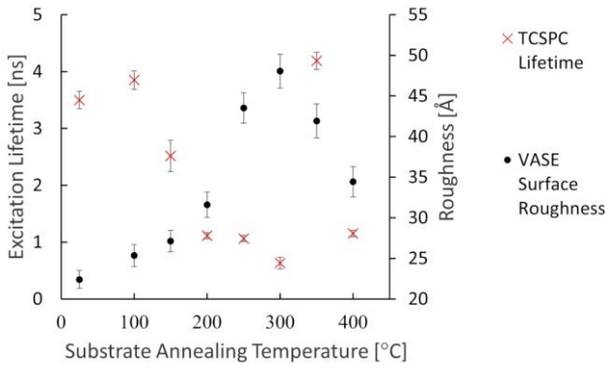

Figure 6: An overlayed graph displaying the PL lifetime and the previously reported surface roughness data. The Biexponential fitting of TCSPC decay curves show a marked change for the amplitude average lifetime of the charge carriers for differently treated substrates. Data points for temperatures below 300 °C show a continually decreasing PL lifetime corresponding to the increased surface roughness. Data points above 300 °C show a discontinuity from this behavior with samples at 350 °C displaying the longest observed PL lifetime.

The observed decrease in PL lifetime with increasing surface roughness is consistent with other reports regarding interfacial effects on charge carrier recombination.[13,14] Studies have demonstrated that surface roughness increases the number of defect sites that act as non-radiative recombination centers, leading to faster carrier recombination.[8,12] Our findings align with these studies, confirming that interface engineering plays a pivotal role in optimizing charge carrier dynamics in perovskite materials. However, the observed discontinuity at higher annealing temperatures (350 °C and 400 °C) presents a unique finding attributed to the onset of recrystallization in the TiO_2 substrates, which has not been extensively reported in previous literature. Exploring the transition from rough amorphous surfaces to smoother, partially recrystallized anatase TiO_2 phases, addresses a gap in understanding how both surface morphology and crystallinity affect charge carrier recombination in perovskite-based devices.

The partial recrystallization of the anatase phase observed at 350 °C significantly improves the PL lifetime, increasing from 0.4 ns at 300 °C to 4.19 ns at 350 °C suggesting that a delicate balance between surface roughness and crystallinity optimizes charge carrier dynamics.

The recrystallization of the TiO_2 substrate at higher annealing temperatures reduces the density of surface defect states, which are known to act as recombination centers for charge carriers. As the anatase phase begins to form at temperatures above 300 °C, the smoother surface and increased crystallinity cause a reduction in defect sites, allowing for more efficient electron transport across the interface of the perovskite/TiO_2 layer. Additionally, the transition to a more ordered crystalline phase reduces the scattering of charge carriers, further contributing to the observed increase in PL lifetime.

D. Implications for Perovskite-Based Devices

The observed correlation between substrate modification and PL lifetime has significant implications for the development of perovskite-based optoelectronic devices. Shorter PL lifetimes, as seen on substrates annealed at

higher temperatures, are indicative of faster charge carrier recombination resulting in decreased performance in devices such as solar cells and LEDs. These results show that optimizing substrate properties through controlled annealing enhances device efficiency and stability.

At 350 °C, the longest photoluminescent (PL) lifetime (4.19 ns) was observed, which is attributed to partial recrystallization of the anatase phase. This annealing condition strikes a balance between surface roughness and crystallinity, reducing non-radiative recombination centers while promoting efficient charge transfer. The partially crystalline surface at 350 °C optimizes the perovskite-substrate interface, enabling slower recombination processes. For perovskite-based devices, this can significantly improve performance, suggesting that controlled annealing to achieve partial recrystallization is an effective strategy for enhancing device efficiency in both photovoltaics and light-emitting applications.

V. SUMMARY AND CONCLUSIONS

In this study, the effects of substrate modifications on the excited state lifetimes of $CsPbBr_3$ perovskites deposited on TiO_2 substrates were investigated. By annealing the TiO_2 substrates at different temperatures ranging from room temperature to 400 °C, we systematically examined how changes in surface roughness and crystallinity influenced the optoelectronic properties of the perovskite microcrystals at the substrate interface. TCSPC spectroscopy was employed to measure the PL lifetimes, and surface characterization techniques such as GAXRD and VASE were used to assess the morphological properties of the substrates.

The results demonstrated a clear correlation between substrate annealing temperature and the PL lifetime of the perovskites. Results indicate that at annealing temperatures ranging from room temperature to 300 °C, there is a clear relationship between substrate annealing temperature and perovskite PL lifetime. Observing the surface roughness data and the reported PL lifetime data we can conclude that an increasing surface roughness corresponds to a decreased PL lifetime. Results indicate that a rougher substrate layer is correlated to shorter amplitude average PL lifetimes due to the rougher surface introducing more surface defects and trap states at the perovskite-substrate interface. These defects act as non-radiative recombination centers where charge carriers can quickly recombine. As a result, the increased surface roughness leads to faster recombination thereby shortening the amplitude average lifetime.

Substrates annealed at higher temperatures, 350 °C and 400 °C, exhibited a discontinuity in the excited state lifetime behavior when compared to samples treated at intermediate temperatures. Substrates annealed at these temperatures exhibit some degree of anatase phase recrystallization. Therefore, alterations to surface roughness are no longer the only variable that is affecting the PL lifetime and recrystallization of the anatase phase is now a contributing factor. Samples treated at 350 °C provided the longest PL lifetime with partial anatase recrystallization. Indicating that, along with surface roughness, the degree of recrystallization of the anatase phase plays an important role in the determination of the charge carrier excitation lifetime at the perovskite-substrate interface, and that some degree of anatase recrystallization should enhance the efficiency of charge carrier dynamics of perovskite-substrate interfaces.

These findings highlight the importance of substrate morphological properties in determining the performance of perovskite-based devices. By reducing surface roughness and promoting crystallization, the substrates provide a more favorable environment for efficient charge carrier transfer and reduced recombination, leading to longer excited state lifetimes. The ability to control excitation lifetime through substrate modifications offers

a promising avenue for optimizing the optoelectronic performance of perovskites, particularly in applications such as photovoltaics and light-emitting devices, where charge carrier lifetime is critical to device efficiency.

In conclusion, this work provides valuable insights into the role of substrate engineering in the development of high-performance perovskite-based technologies. By demonstrating how annealing conditions affect both the morphological and optoelectronic properties of perovskite-substrate interfaces, providing the groundwork for future research aimed at further optimizing perovskite materials for a wide range of optoelectronic applications. Future work will involve exploring additional substrate modifications and their effects on other key performance metrics, such as charge mobility and charge carrier density.

VI. SUPPLEMENTAL MATERIAL

The supplementary material provides additional data and analyses supporting this study. It includes details on the characterization of TiO_2 substrate roughness using variable angle spectroscopic ellipsometry, elemental composition analysis of perovskite microcrystals using SEM-EDS, identification of crystalline phases through X-ray diffraction, and time-resolved photoluminescence decay data. These materials offer further insights into the morphological and optoelectronic properties of the perovskite systems studied.

VII. ACKNOWLEDGMENTS

Research was sponsored by the Combat Capabilities Development Command Army Research Laboratory and was accomplished under Cooperative Agreement No. W911NF-15-2-0020. The views and conclusions contained in this document are those of the authors and should not be interpreted as representing the official policies, either expressed or implied, of the Army Research Laboratory or the U.S. Government. The U.S. Government is authorized to reproduce and distribute reprints for Government purposes notwithstanding any copyright notation herein.

VIII. Author Declarations

The authors have no conflicts of interest to disclose.

IX. Data Availability

The data that support the findings of this study are available from the corresponding author upon reasonable request.

X. References

[1] N. S. Kumar and K. C. B. Naidu, *J. Materiomics* **7**, 940 (2021).
[2] S. Pitchaiya, M. Natarajan, A. Santhanam, V. Asokan, A. Yuvapragasam, V. M. Ramakrishnan, S. E. Palanisamy, S. Sundaram, and D. Velauthapillai, *Arab. J. Chem.* **13**, 2526 (2020).
[3] I. Mesquita, L. Andrade, and A. Mendes, *Renew. Sust. Energ. Rev.* **82**, 2471 (2018).
[4] A. Aftab and M. I. Ahmad, *Sol. Energy* **216**, 26 (2021).
[5] S. D. Stranks and H. J. Snaith, *Nat. Nanotechnol.* **10**, 391 (2015).
[6] I. J. Djeukeu, J. Horn, M. Meixner, E. Wagner, S. W. Glunz, and K. Ramspeck, *Sol. RRL*, (2024).
[7] Y. Hou, W. Chen, D. Baran, T. Stubhan, N. A. Luechinger, B. Hartmeier, M. Richter, J. Min, S. Chen, C. O. R. Quiroz, N. Li, H. Zhang, T. Heumueller, G. J. Matt, A. Osvet, K. Forberich, Z. G. Zhang, Y. Li, B. Winter, P. Schweizer, E. Spiecker, and C. J. Brabec, *Adv. Mater.* **28**, 5112 (2016).
[8] J. M. Marin-Beloqui, L. Lanzetta, and E. Palomares, *Chem. Mater.* **28**, 207 (2016).
[9] W. Tress, M. Yavari, K. Domanski, P. Yadav, B. Niesen, J. P. Correa Baena, A. Hagfeldt, and M. Graetzel, *Energy Environ. Sci.* **11**, 151 (2018).
[10] J. W. Lee, T. Y. Lee, P. J. Yoo, M. Grätzel, S. Mhaisalkar, and N. G. Park, *J. Mater. Chem. A* **2**, 9251 (2014).
[11] J. Dou and Q. Chen, *Energy Mater. Adv.* **2022**, (2022).
[12] L. P. Cheng, J. S. Huang, Y. Shen, G. P. Li, X. K. Liu, W. Li, Y. H. Wang, Y. Q. Li, Y. Jiang, F. Gao, C. S. Lee, and J. X. Tang, *Adv. Opt. Mater.* **7**, (2019).
[13] T. P. Weiss, B. Bissig, T. Feurer, R. Carron, S. Buecheler, and A. N. Tiwari, *Sci. Rep.* **9**, (2019).
[14] G. Yang, H. Tao, P. Qin, W. Ke, and G. Fang, *J. Mater. Chem. A* **4**, 3970 (2016).
[15] A. B. Djurišić, F. Z. Liu, H. W. Tam, M. K. Wong, A. Ng, C. Surya, W. Chen, and Z. B. He, *Prog. Quant. Electron.* **53**, 1 (2017).
[16] K. Ye, B. Zhao, B. T. Diroll, J. Ravichandran, and R. Jaramillo, *Faraday Discuss.* **239**, 146 (2022).
[17] E. V. Peán, S. Dimitrov, C. S. De Castro, and M. L. Davies, *Phys. Chem. Chem. Phys.* **22**, 28345 (2020).
[18] C. Y. Huang, C. C. Wu, C. L. Wu, and C. W. Lin, *ACS Omega* **4**, 8081 (2019).
[19] D. N. Dirin, I. Cherniukh, S. Yakunin, Y. Shynkarenko, and M. V. Kovalenko, *Chem. Mater.* **28**, 8470 (2016).
[20] A. W. Faridi, M. Imran, G. H. Tariq, S. Ullah, S. F. Noor, S. Ansar, and F. Sher, *Ind. Eng. Chem. Res.* **62**, 4494 (2023).
[21] Y. Cho, H. R. Jung, and W. Jo, *Nanoscale* **14**, 9248 (2022).
[22] Z. Lai, Y. Meng, F. Wang, X. Bu, W. Wang, P. Xie, W. Wang, C. Liu, S. P. Yip, and J. C. Ho, *Nano Res.* **15**, 3621 (2022).